

12
B3

LEVEL III

AD-E430497

AD

AD A 089982

TECHNICAL REPORT ARBRL-TR-02248

A PROBLEM IN NUCLEAR THERMAL
RADIATION ENVIRONMENT SIMULATION
FOR SYSTEM SURVIVABILITY

Ennis F. Quigley
John M. Evans

August 1980

DTIC
ELECTE
OCT 7 1980
S D
B



US ARMY ARMAMENT RESEARCH AND DEVELOPMENT COMMAND
BALLISTIC RESEARCH LABORATORY
ABERDEEN PROVING GROUND, MARYLAND

Approved for public release; distribution unlimited.

DDC FILE COPY

80 9 29 131

Destroy this report when it is no longer needed.
Do not return it to the originator.

Secondary distribution of this report by originating
or sponsoring activity is prohibited.

Additional copies of this report may be obtained
from the National Technical Information Service,
U.S. Department of Commerce, Springfield, Virginia
22151.

The findings in this report are not to be construed as
an official Department of the Army position, unless
so designated by other authorized documents.

*The use of trade names or manufacturers' names in this report
does not constitute indorsement of any commercial product.*

UNCLASSIFIED

SECURITY CLASSIFICATION OF THIS PAGE (When Data Entered)

REPORT DOCUMENTATION PAGE		READ INSTRUCTIONS BEFORE COMPLETING FORM
1. REPORT NUMBER Technical Report ARBRL-TR-02248	2. GOVT ACCESSION NO. AD-A089982	3. RECIPIENT'S CATALOG NUMBER
4. TITLE (and Subtitle) A PROBLEM IN NUCLEAR THERMAL RADIATION ENVIRONMENT SIMULATION FOR SYSTEM SURVIVABILITY	5. TYPE OF REPORT & PERIOD COVERED FINAL	
	6. PERFORMING ORG. REPORT NUMBER	
7. AUTHOR(s) Ennis F. Quigley and John M. Evans	8. CONTRACT OR GRANT NUMBER(s)	
9. PERFORMING ORGANIZATION NAME AND ADDRESS US Army Ballistic Research Laboratory ✓ ATTN: DRDAR-BLV Aberdeen Proving Ground, MD 21005	10. PROGRAM ELEMENT, PROJECT, TASK AREA & WORK UNIT NUMBERS IW162118AH75	
11. CONTROLLING OFFICE NAME AND ADDRESS US Army Armament Research & Development Command US Army Ballistic Research Laboratory ATTN: DRDAR-BL Aberdeen Proving Ground, MD 21005	12. REPORT DATE August 1980	
	13. NUMBER OF PAGES 58	
14. MONITORING AGENCY NAME & ADDRESS (if different from Controlling Office)	15. SECURITY CLASS. (of this report)	
	UNCLASSIFIED 15a. DECLASSIFICATION DOWNGRADING SCHEDULE	
16. DISTRIBUTION STATEMENT (of this Report) Approved for public release; distribution unlimited.		
17. DISTRIBUTION STATEMENT (of the abstract entered in Block 20, if different from Report)		
18. SUPPLEMENTARY NOTES		
19. KEY WORDS (Continue on reverse side if necessary and identify by block number) Nuclear Thermal Radiation Simulation Simulator Spectrum Forest Green Camouflage Paint Thermal Flux		
20. ABSTRACT (Continue on reverse side if necessary and identify by block number) A series of experiments was conducted at two nuclear thermal radiation simulators; the White Sands Missile Range Solar Furnace facility and the Wright-Patterson Air Force Base Quartz Lamps facility. The purpose of these experiments was to study the effect of simulator radiation spectrum on the amount of thermal energy absorbed by painted surfaces. The results of the experiments show that the amount of thermal energy absorbed is highly dependent on the thermal radiation spectrum. Thirty-nine percent more energy was absorbed using the solar furnace than was absorbed using the quartz lamps. The experimental		

DD FORM 1473 EDITION OF 1 NOV 65 IS OBSOLETE

UNCLASSIFIED
SECURITY CLASSIFICATION OF THIS PAGE (When Data Entered)

UNCLASSIFIED

SECURITY CLASSIFICATION OF THIS PAGE(When Data Entered)

results also indicated that the amount of absorbed energy may be independent of of thermal radiation flux.

UNCLASSIFIED

SECURITY CLASSIFICATION OF THIS PAGE(When Data Entered)

TABLE OF CONTENTS

	Page
LIST OF ILLUSTRATIONS.....	5
LIST OF TABLES.....	7
I. INTRODUCTION.....	9
II. PROCEDURE.....	10
III. RESULTS AND DISCUSSION.....	13
IV. CONCLUSIONS.....	29
APPENDIX A.....	31
DISTRIBUTION LIST.....	37

S DTIC
 ELECTE **D**
 OCT 7 1980
B

Accession For	
NTIS GRA&I	<input checked="" type="checkbox"/>
NTIS GPO	<input type="checkbox"/>
NTIS PC	<input type="checkbox"/>
Availability Codes	
Dist	Special
A	

LIST OF ILLUSTRATIONS

Figure	Page
1. Solar Furnace Flux Distribution at Focal Plane.....	12
2. Average Temperature Data of all Samples - Quartz Lamps.	14
3. Average Temperature Data of all Samples - Quartz Lamps.	15
4. Sample A Average Temperatures - Quartz Lamps.....	16
5. Sample B Average Temperatures - Quartz Lamps.....	17
6. Sample C Average Temperatures - Quartz Lamps.....	18
7. Sample D Average Temperatures - Quartz Lamps.....	19
8. Sample E Average Temperatures - Quartz Lamps.....	20
9. Average Temperature Data of all Samples - Solar Furnace.....	22
10. Average Temperature Data of all Samples - Solar Furnace.....	23
11. Sample A Average Temperatures - Solar Furnace.....	24
12. Sample B Average Temperatures - Solar Furnace.....	25
13. Sample C Average Temperatures - Solar Furnace.....	26
14. Sample D Average Temperatures - Solar Furnace.....	27
15. Sample E Average Temperatures - Solar Furnace.....	28

LIST OF TABLES

Table	Page
1. Forest Green Camouflage Paint-Primer Samples.....	11
2. Simulator Pulse Characteristics.....	11
3. Effective Absorptivity for Quartz Lamps Source.....	13
4. Effective Absorptivity for Solar Furnace Source.....	21
5. Effective Absorptivity.....	29
A1. Number of Paint-Primer Exposures.....	31
A2. Average Temperatures for Quartz Lamps.....	32
A3. Average Temperatures for Quartz Lamps.....	33
A4. Average Temperatures for Solar Furnace.....	34
A5. Average Temperatures for Solar Furnace.....	35

I. INTRODUCTION

Until the middle of 1977 the survivability testing of full scale US Army tactical systems to simulated nuclear thermal environments and to combined nuclear thermal-blast environments was not possible. Since that time Scientific Applications, Inc., under contract to the Defense Nuclear Agency, has been developing a general purpose thermal radiation simulator¹ which may provide the means for such testing. This simulator is transportable and self-consuming and can be used to irradiate targets ranging in sizes from laboratory models to full-size prototypes. The thermal radiation is produced by the burning of aluminum powder in an oxygen atmosphere at a temperature of approximately 3600° K. This simulator has been used by the Ballistic Research Laboratory for nuclear thermal survivability studies of several Lance Missile System components and for combined nuclear thermal-blast survivability studies of C³ systems. Since there now exists the possibility to conduct thermal and thermal-blast survivability testings of large tactical systems, it is necessary to determine those characteristics of the nuclear thermal radiation environment which must be simulated in order to obtain valid results from such tests.

The effects of the thermal environment on a system are due to the absorption of all or part of the radiant energy incident on the exposed surfaces. These surfaces are generally painted and the amount of energy absorbed by the system is highly dependent on the thermal radiation absorptivity of the surfaces. To determine to what extent the nuclear thermal environment must be simulated, one must know the characteristics of the environment at the target and the dependence of the thermal absorptivity on these characteristics.

The general characteristics of the nuclear thermal environment at a tactical target are the pulse shape, the rise time of the pulse, the maximum thermal flux, the total thermal fluence, and the time dependent radiation spectrum. Of these five characteristics, only the first four are considered for survivability testing. The fifth characteristic, the radiation spectrum, is never considered because of the inherent difficulties associated with spectral characterization. Consequently, the most difficult characteristic to simulate is then the radiation spectrum. To study the effect of simulator spectrum on the amount of thermal energy absorbed by painted surfaces, a series of experiments have been conducted at two nuclear thermal radiation environment simulators; the White Sands

¹J. F. Dishon, "Large Scale Thermal Radiation Simulator", DNA 001-77-C-0206, 12 May 1977, 1st Monthly Report.

Missile Range (WSMR) Solar Furnace facility² and the Wright-Patterson Air Force Base (WPAFB) Quartz Lamp facility³. This report describes these experiments and their results.

II. PROCEDURE

Assuming that a plate is thermally thin, the amount of thermal energy absorbed by the painted surface is directly proportional to the time derivative of the plate temperature. This functional relationship is:

$$\alpha \dot{Q} = \rho c l \frac{dT}{dt} + H \quad (1)$$

where

α = surface absorptivity

\dot{Q} = thermal flux

ρ = plate density

c = plate specific heat

l = plate thickness

T = plate temperature

t = time

and H = thermal energy losses by the plate

If an effective absorptivity, α_e , is defined such that

$$\alpha_e \dot{Q} = \rho c l \frac{dT}{dt} \quad (2)$$

the difficulties of determining H are avoided. By obtaining α_e for each simulator, one can determine the effect of simulator spectrum on the amount of energy absorbed by painted surfaces.

²White Sands Solar Facility Experimenter's Guide, 1977.

³A. Servois, J. Olson, and H. Hilt, "Tri-Service Thermal Flash Test Facility", DNA 44 88Z, March 1978, University of Dayton, Dayton, OH 4509 (AD-A056 321)

The paint-primer samples which were tested are listed in Table 1.

TABLE 1. Forest Green Camouflage Paint-Primer Samples

Sample	Primer	Paint
A	TT-P-636*	MIL-E-52798A*
B	TT-P-664	MIL-E-52835A
C	TT-P-664	MIL-L-52909
D	TT-P-664	MIL-L-52926
E	TT-P-664	MIL-L-52929

The substrate for each sample was a 50 mm x 50 mm x 1.0 mm ASIS 1020 cold rolled steel plate and the samples were fabricated by the US Army Camouflage Laboratory at Fort Belvoir, VA. One end of a one meter length K-type thermocouple was spot-welded at the center of the back of each plate.

As previously mentioned, the thermal simulators used in the tests were the Quartz Lamp (QL) facility at WPAFB and the Solar Furnace (SF) facility at WSMR. The thermal environment characteristics of the QL were a radiating temperature of approximately 2800°K and a thermal flux which was uniform over the entire surface of the sample. The SF had a radiating temperature of approximately 6000°K and a thermal flux distribution over the sample surface as shown in Figure 1. Calculations were made to determine the effect of a nonuniform, but axial symmetric, flux distribution on the back center temperature of the plate. The results of the calculations showed that the differences between temperatures produced by a uniform flux distribution and the SF flux distribution were less than 1% for the flux values used in the tests. The thermal pulse characteristics for the tests are given in Table 2.

TABLE 2. Simulator Pulse Characteristics

Characteristic	Quartz Lamps	Solar Furnace
Pulse Shape	Rectangular	Rectangular
Thermal Flux	0.84 MW/m ² 1.59 MW/m ²	0.84 MW/m ² 1.63 MW/m ²
Thermal Fluence	2.51 MJ/m ²	2.51 MJ/m ²
Rise Time	t < 30 ms	t < 30 ms

*These numbers refer to the Military Specifications of the primers and paints.

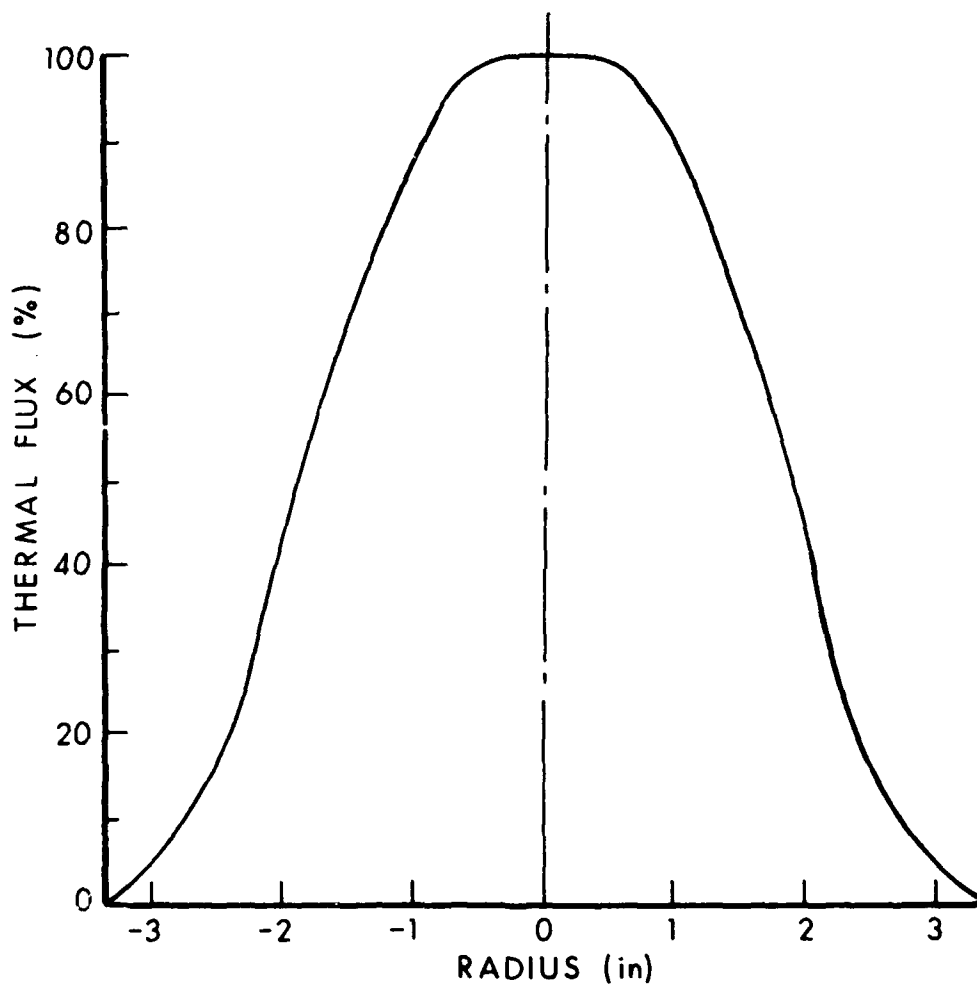


Figure 1. Solar Furnace Flux Distribution at Focal Plane

For the QL tests the output of the thermocouples was recorded on a HP 1360 X-Y recorder; for the SF tests, the thermocouple output was recorded on a Gould 816 strip-chart recorder. Three to five specimens of each paint-primer combination were exposed. Measurement of the thermal flux was performed before and after each set of paint-primer combinations for both simulators.

III. RESULTS AND DISCUSSIONS

Figures 2 and 3 are plots of the average plate temperatures, \bar{T} , of all the samples exposed to the QL simulator for thermal flux values of 0.84 MW/m^2 and 1.59 MW/m^2 , respectively. (For all figures involving \bar{T} , thermal fluence, Q , rather than time was used as the independent parameter since $Q = Qt$.) The plotted data* indicates for each flux that the average temperature response of the plates are approximately the same for each sample and that \bar{T} might be expressible as a linear function of Q . Figures 4 through 8 are plots of the linear regression curve of \bar{T} for each sample. The data and curves in these figures suggest that \bar{T} is independent of the thermal flux value. An effective absorptivity for each sample can be calculated from Equation (2) since $\bar{T} = a+bQ = a+bQt$ and $\frac{d\bar{T}}{dt} = bQ$. The values of p and c used in the calculations are $7.833 \times 10^5 \text{ kg/m}^3$ and $465 \text{ J/kg}^\circ\text{K}$, respectively. The values of α_e are given in Table 3 where $\bar{\alpha}_e$ is the average effective absorptivity of all the samples for that flux value.

TABLE 3. Effective Absorptivity for Quartz Lamps Source

Sample	Flux = 0.84 MW/m^2	Flux = 1.59 MW/m^2
A	0.48	0.43
B	0.47	0.46
C	0.45	0.45
D	0.50	0.49
E	0.45	0.44
$\bar{\alpha}_e$	0.47 ± 0.02	0.45 ± 0.05

*See Appendix A for tabulated data.

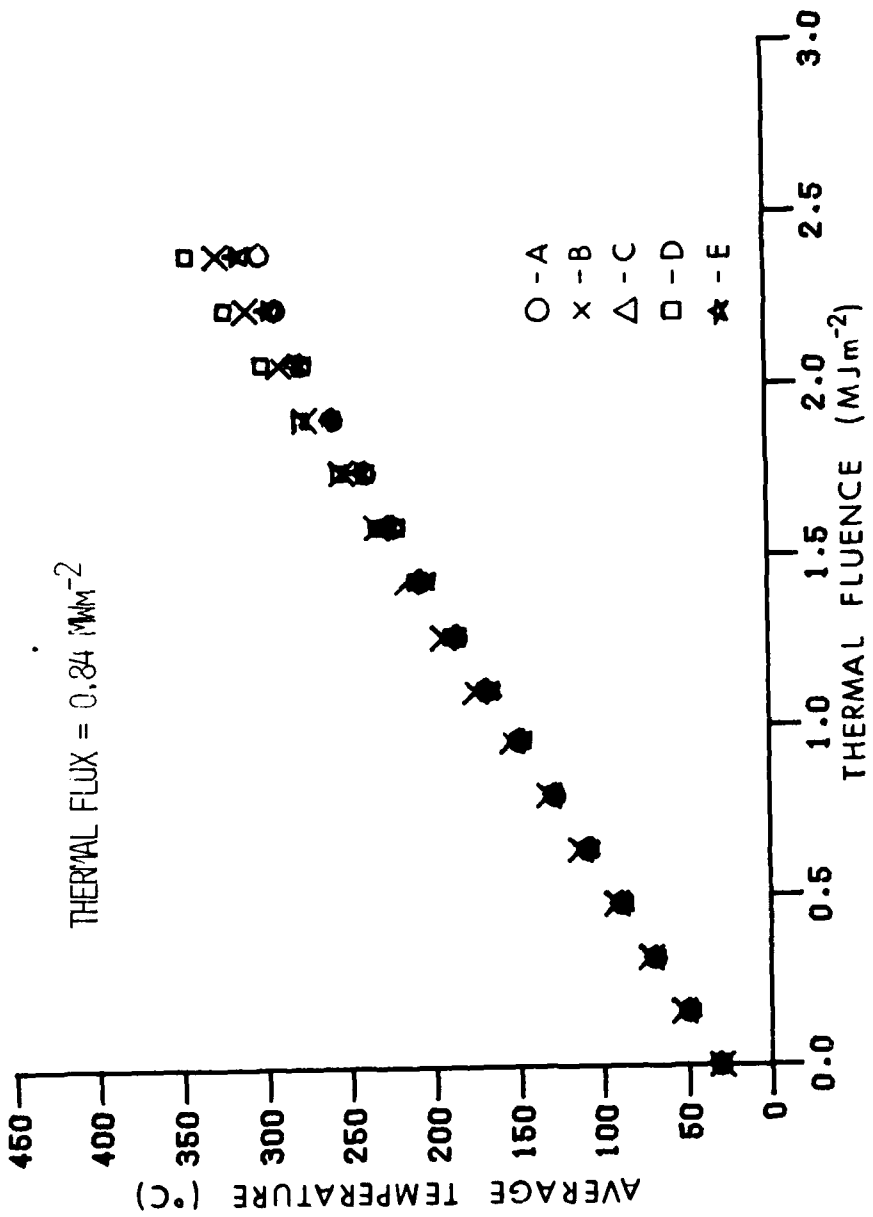


Figure 2. Average Temperature Data of all Samples - Quartz Lamps

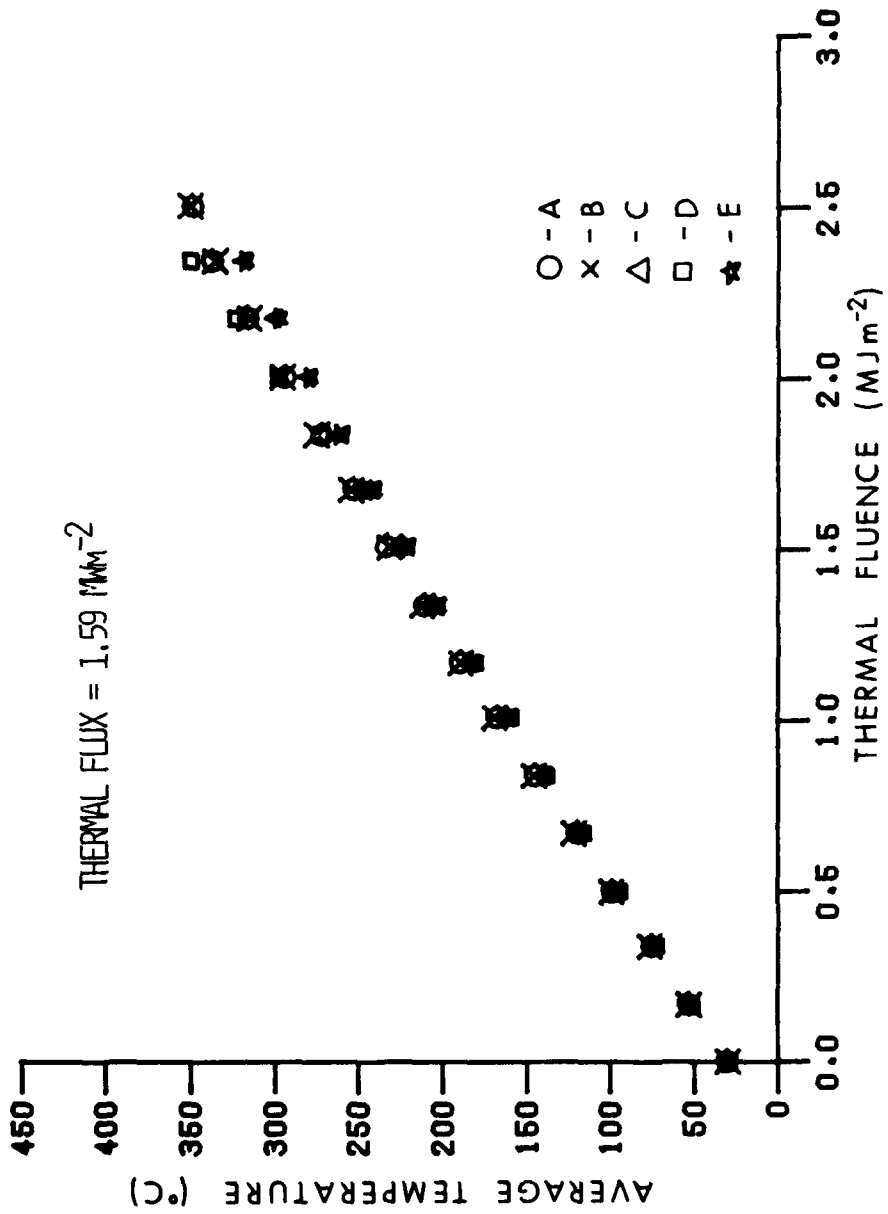


Figure 3. Average Temperature Data of all Samples - Quartz Lamps

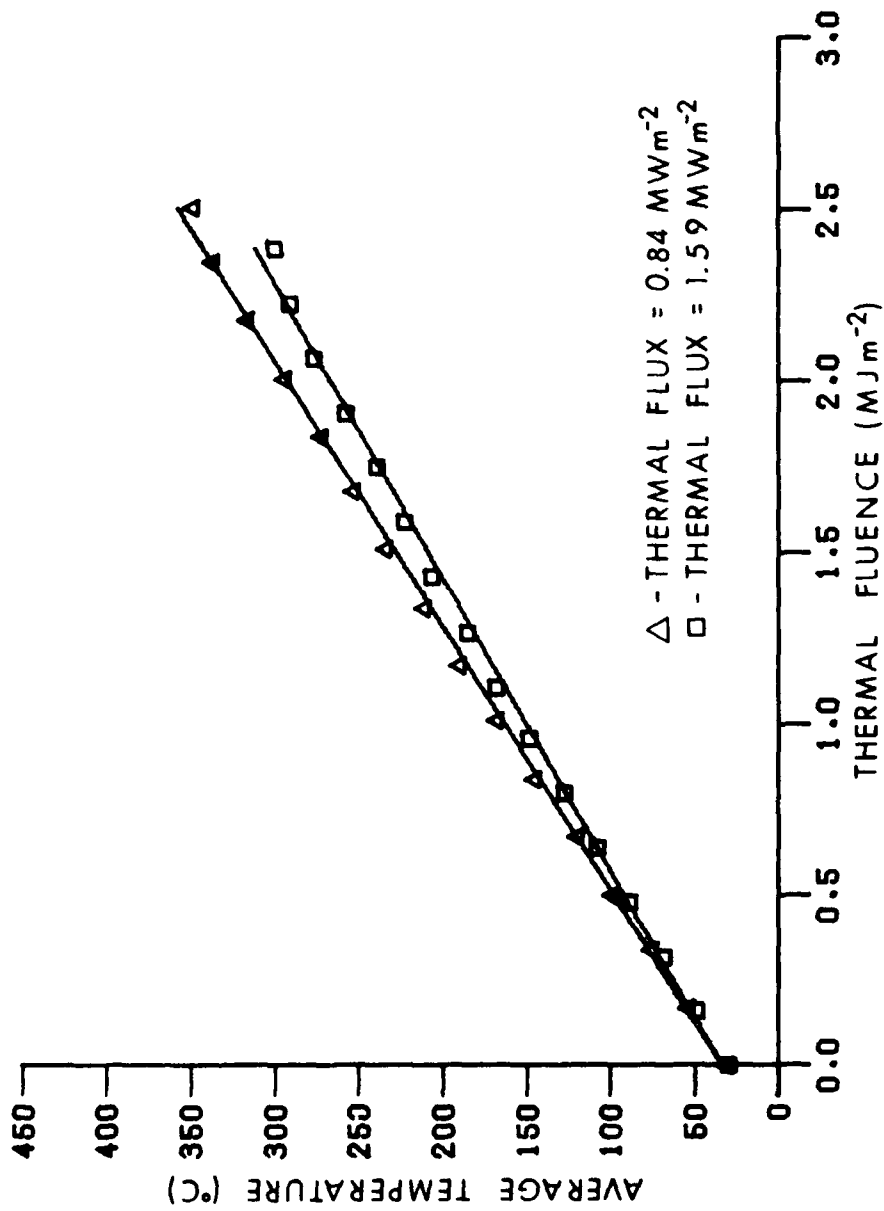


Figure 4. Sample A Average Temperature - Quartz Lamps

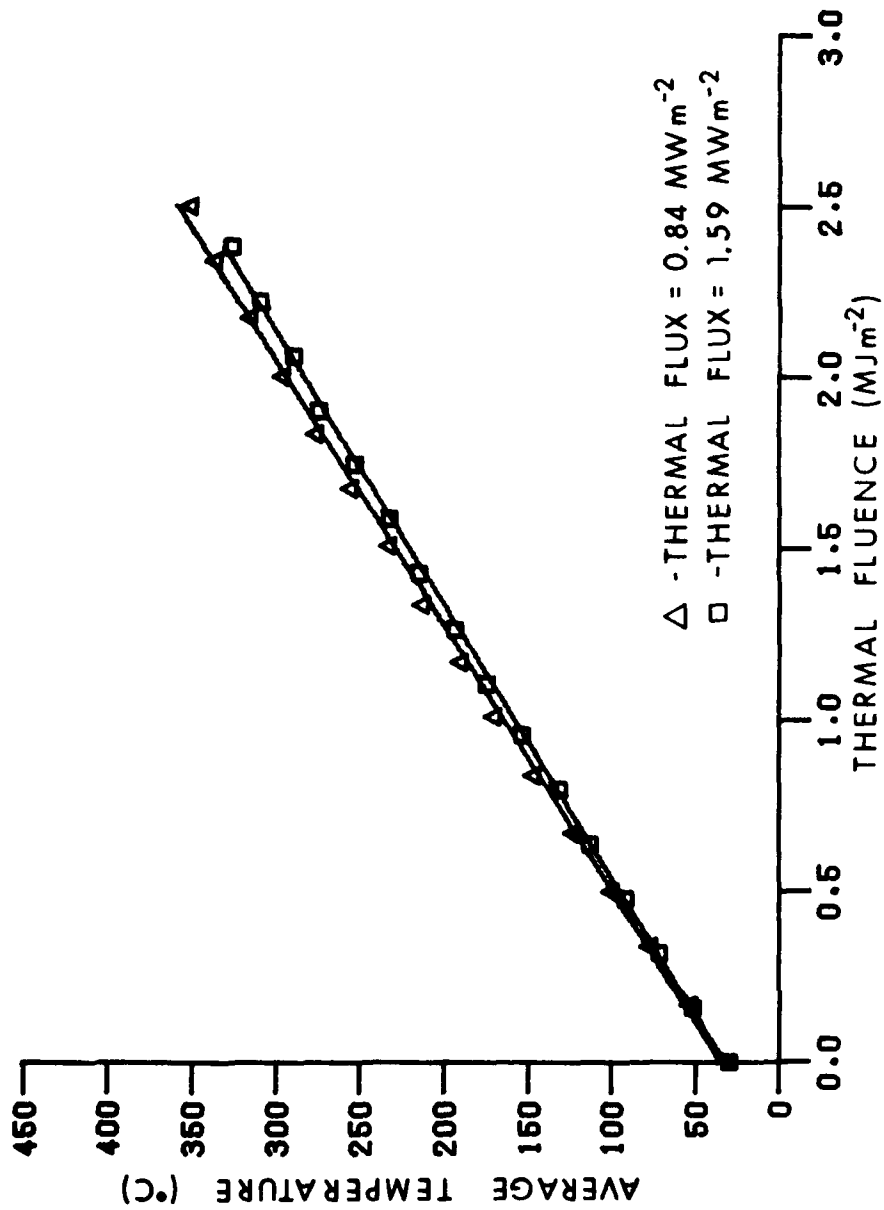


Figure 5. Sample B Average Temperature - Quartz Lamps

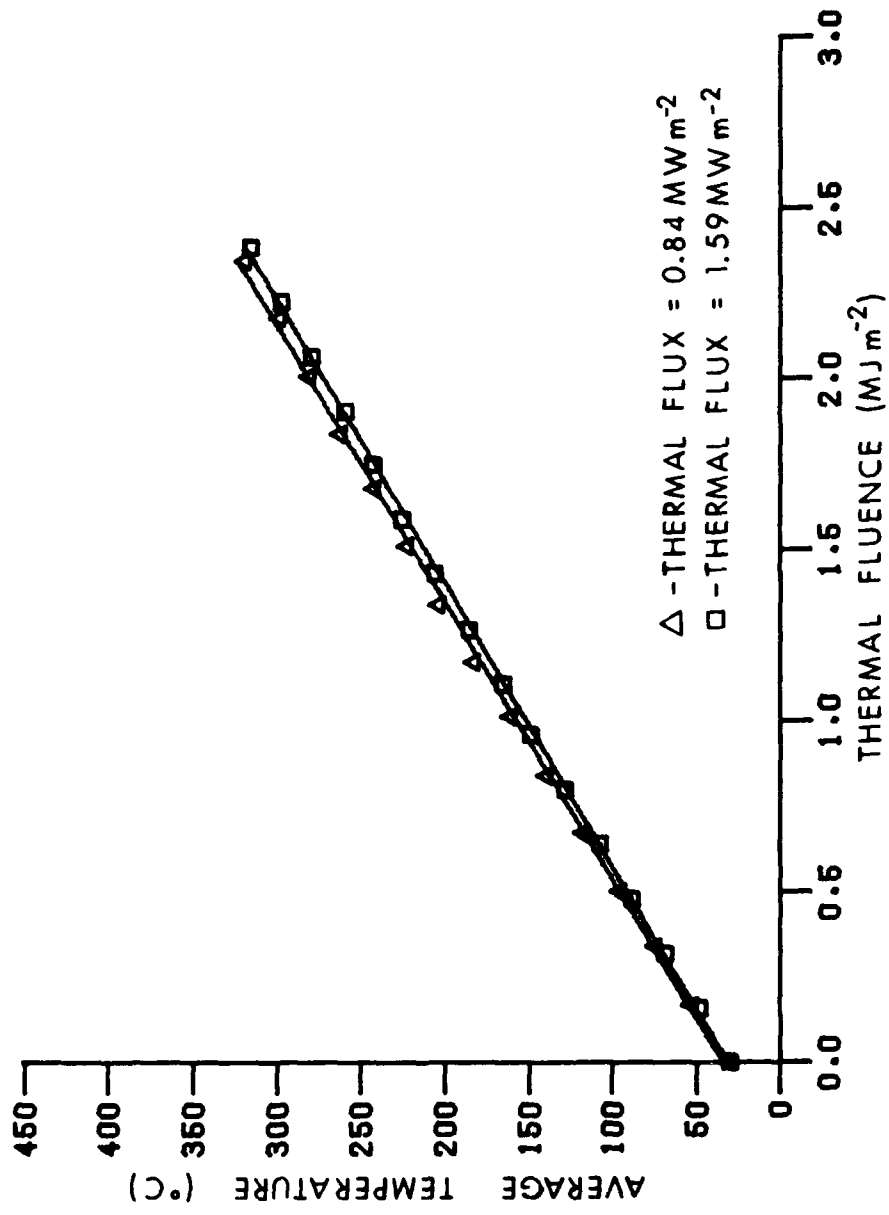


Figure 6. Sample C Average Temperature - Quartz Lamps

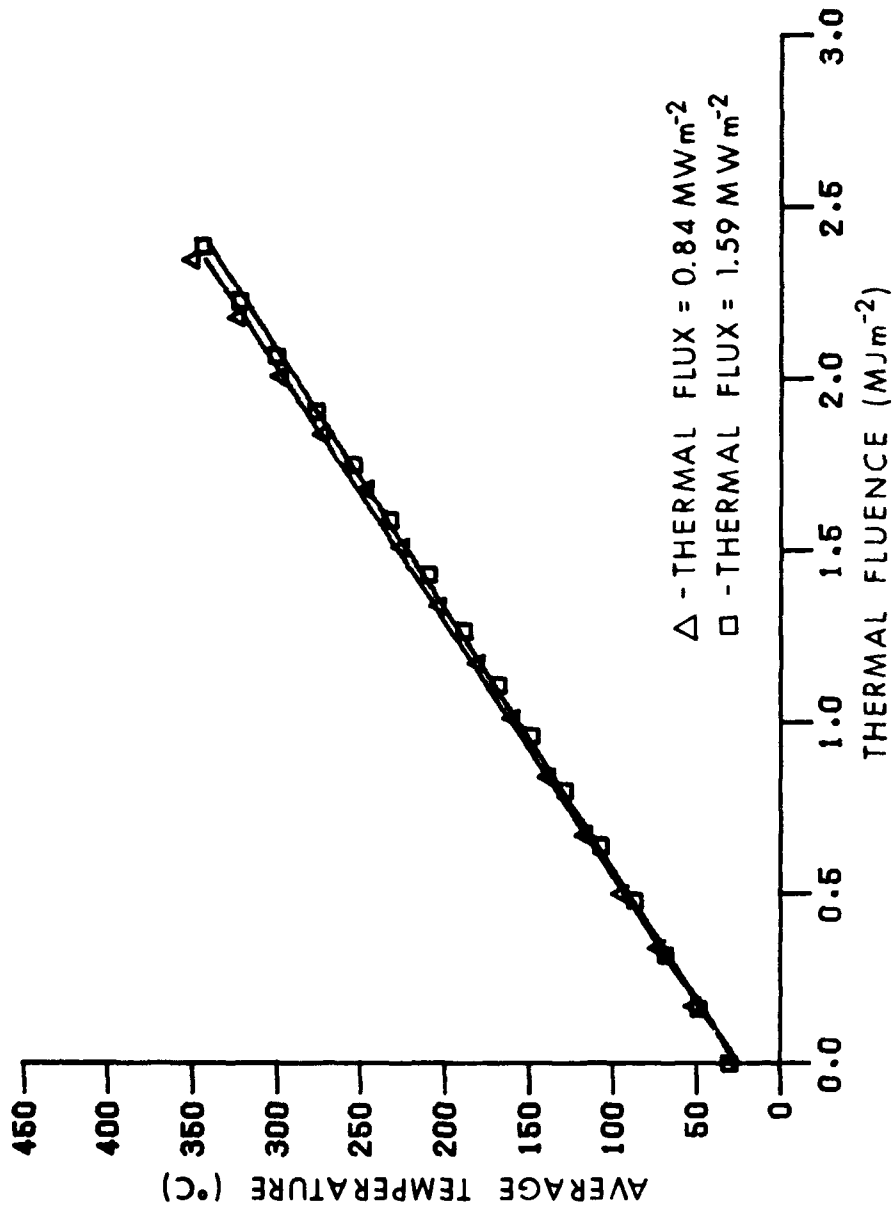


Figure 7. Sample B Average Temperature - Quartz Lamps

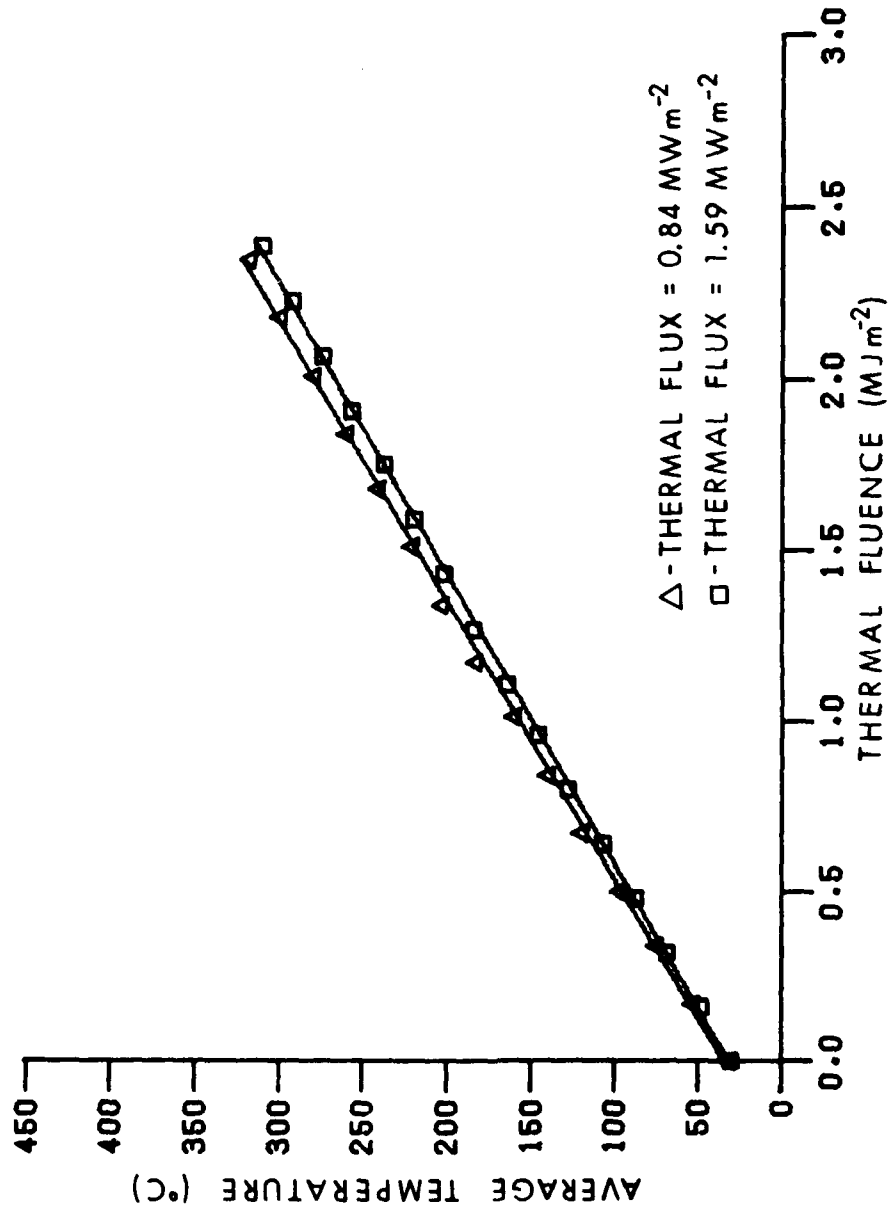


Figure 8. Sample F: Average Temperature - Quartz Lamps

It can be concluded from the test data that the effective absorptivities for all the Forest Green Camouflage paint-primer combination have the same value, can be considered independent of temperature for temperatures less than 300° C, and may be independent of the thermal flux for the QL simulator.

Figures 9 and 10 are plots of \bar{T} for values of Q of all the samples for the SF simulator for thermal flux values of 0.84 MW/m² and 1.63 MW/m², respectively. The data* in Figure 9 indicates for T < 300°C that the average temperature response of the plates for each sample are approximately the same and that \bar{T} could be expressed as a linear function of Q. For \bar{T} > 300°C, samples B, C, and D show similar temperature behavior and samples A and E show similar temperature behavior. Physical examination of samples A and E immediately following exposure revealed that all or most of the paint had been burnt off. The data* in Figure 10 indicates for \bar{T} < 200°C that the average temperature response of each sample is approximately the same and that \bar{T} could be expressed as a linear function of Q. For T > 200°C, samples B and C show similar temperature behavior and samples A and F show similar temperature behavior. Sample D for this flux value did not behave like sample B and C; but more like samples A and E. The reason for this is not clear. After exposure, samples A and F had all or most of the paint burnt off. Figures 11 through 15 are plots of the regression curve and data for each sample. Each curve ends at the last data point used in obtaining the curve. The data and curves in these figures suggest that \bar{T} is independent of the flux value for all measured temperatures. The data also indicates that for \bar{T} > 500°C, the \bar{T} of each sample could be expressed as a linear function of Q. The calculated $\bar{\alpha}_e$ of each sample is given in Table 4 where $\bar{\alpha}_e$ is the average effective absorptivity of all the samples for that flux value.

TABLE 4. Effective Absorptivity for Solar Furnace Source

Sample	Flux = 0.84 MW/m ²	Flux = 1.63 MW/m ²
A	0.64	0.62
B	0.67	0.64
C	0.66	0.64
D	0.65	0.61
E	0.66	0.61
$\bar{\alpha}_e$	0.66 ± 0.01	0.62 ± 0.02

*See Appendix A for tabulated data.

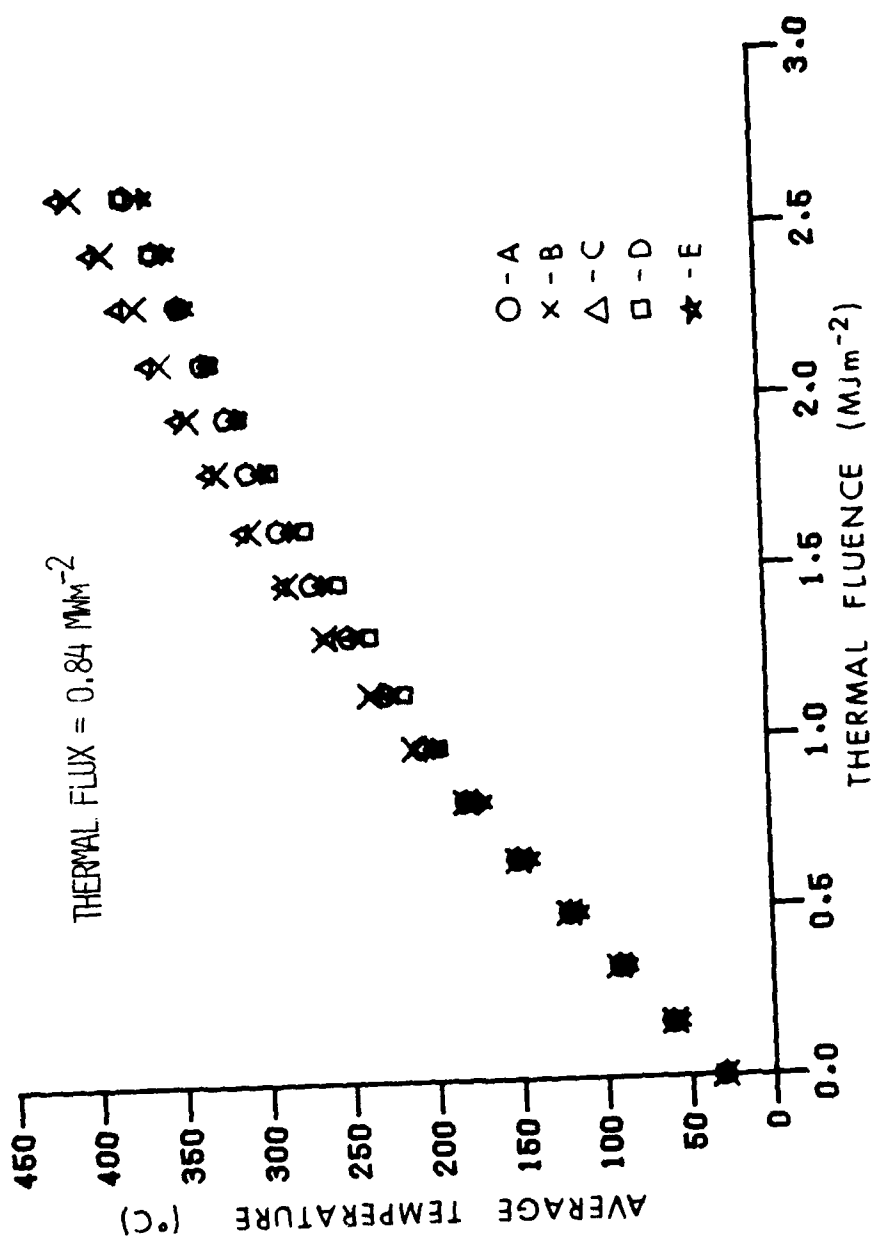


Figure 9. Average Temperature Data of all Samples - Solar Furnace

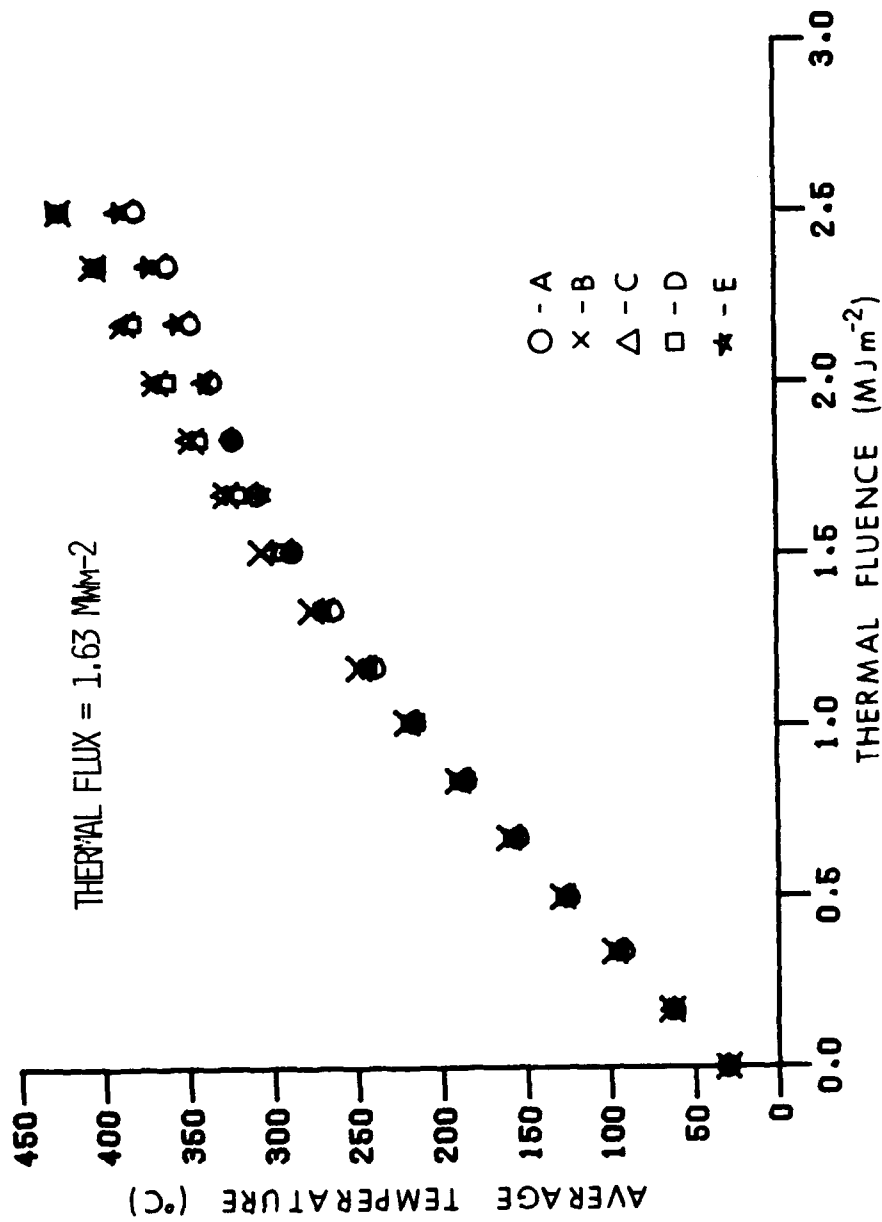


Figure 10. Average Temperature Data of all Samples - Solar Furnace

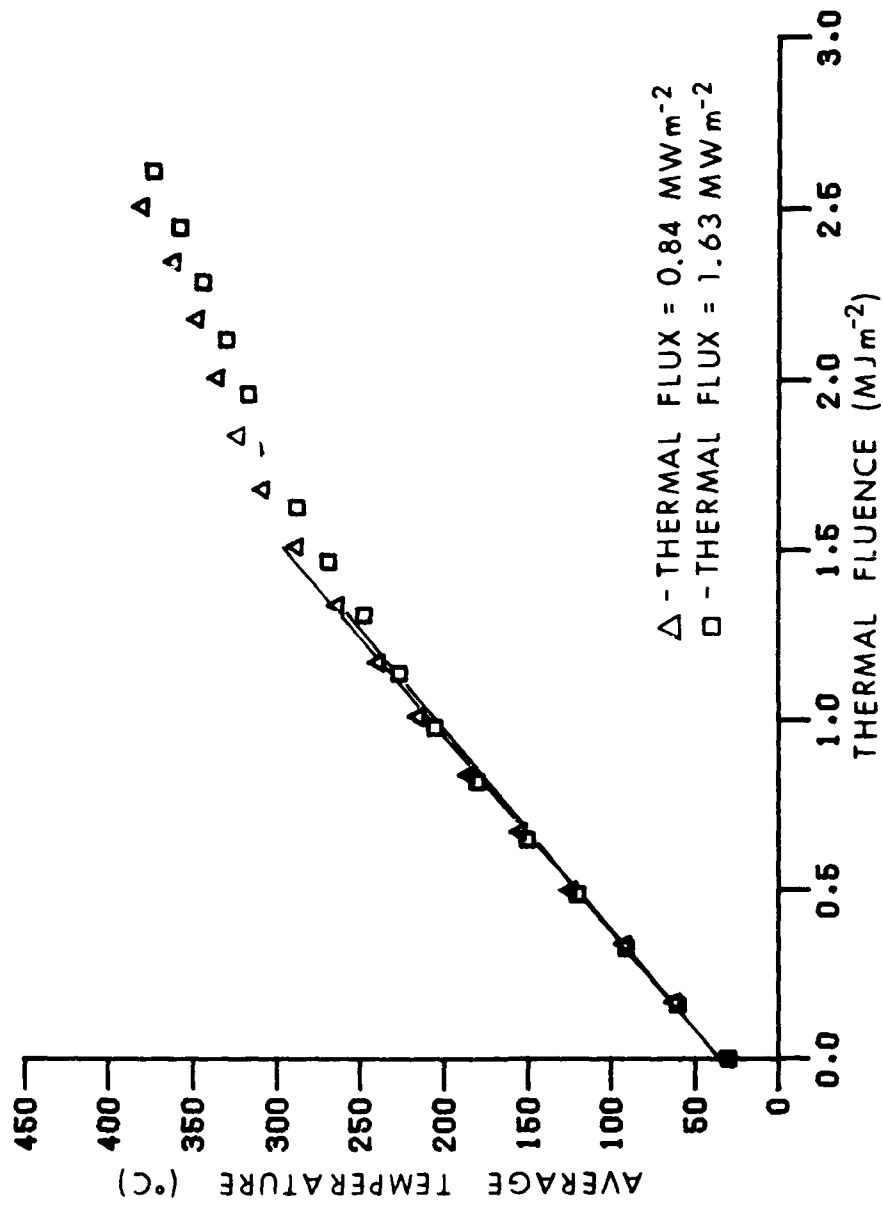


Figure 11. Sample A Average Temperature - Solar Furnace

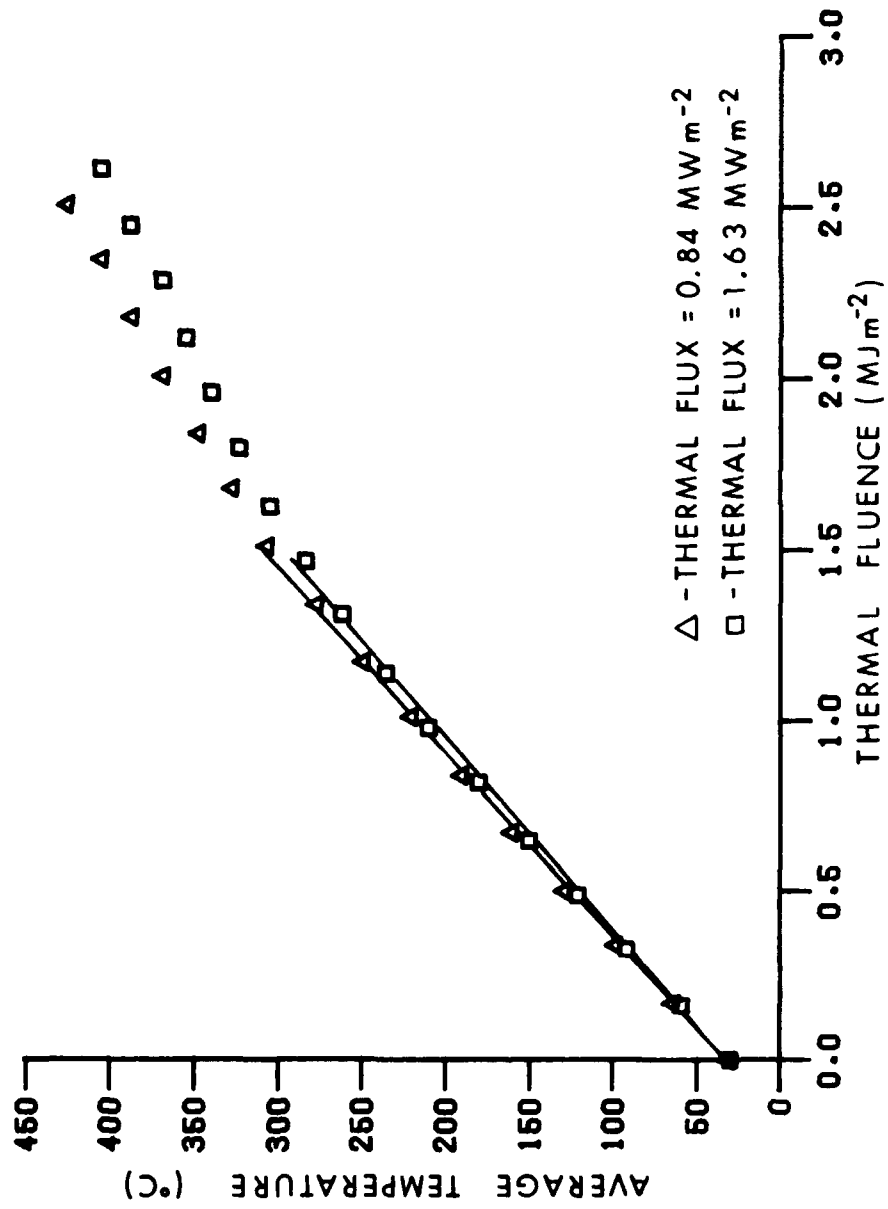


Figure 12. Sample B Average Temperature - Solar Furnace

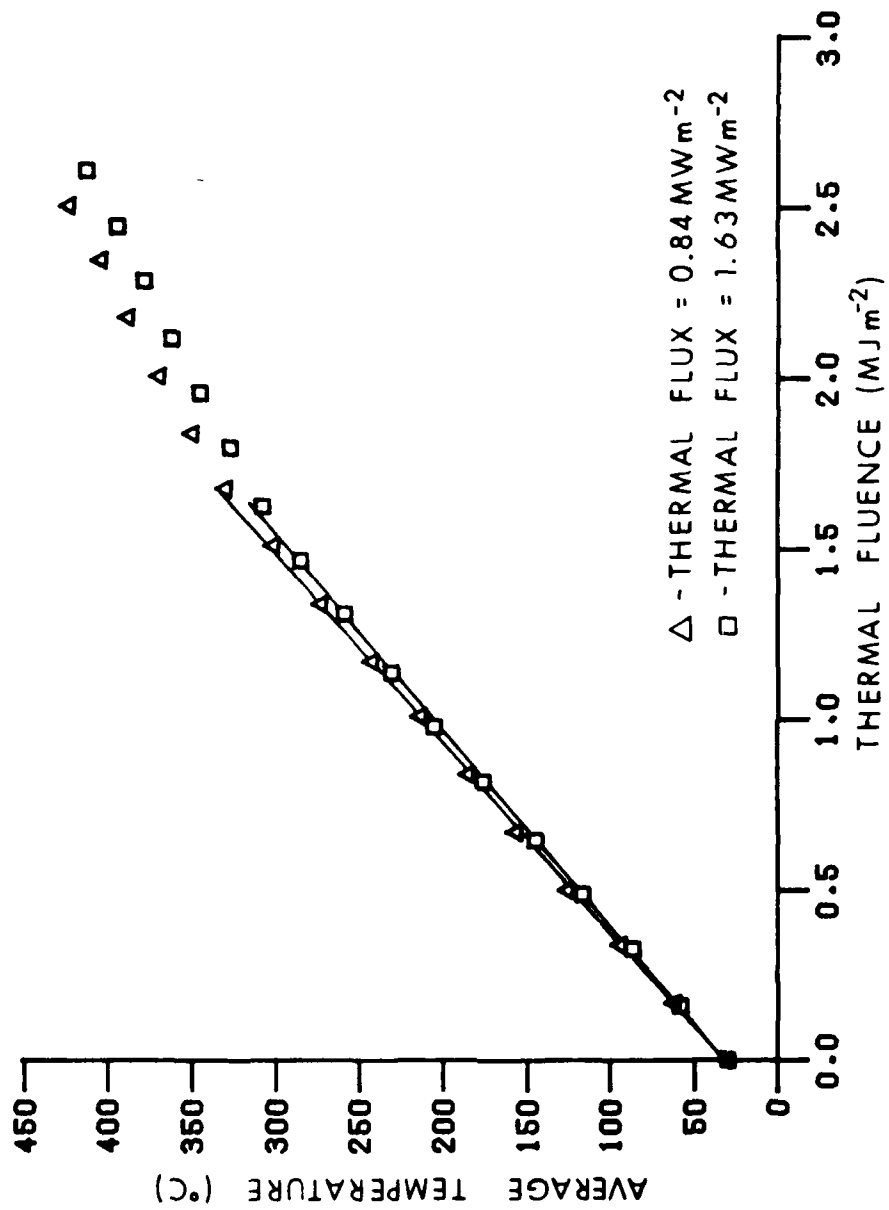


Figure 15. Sample C Average Temperature - Solar Furnace

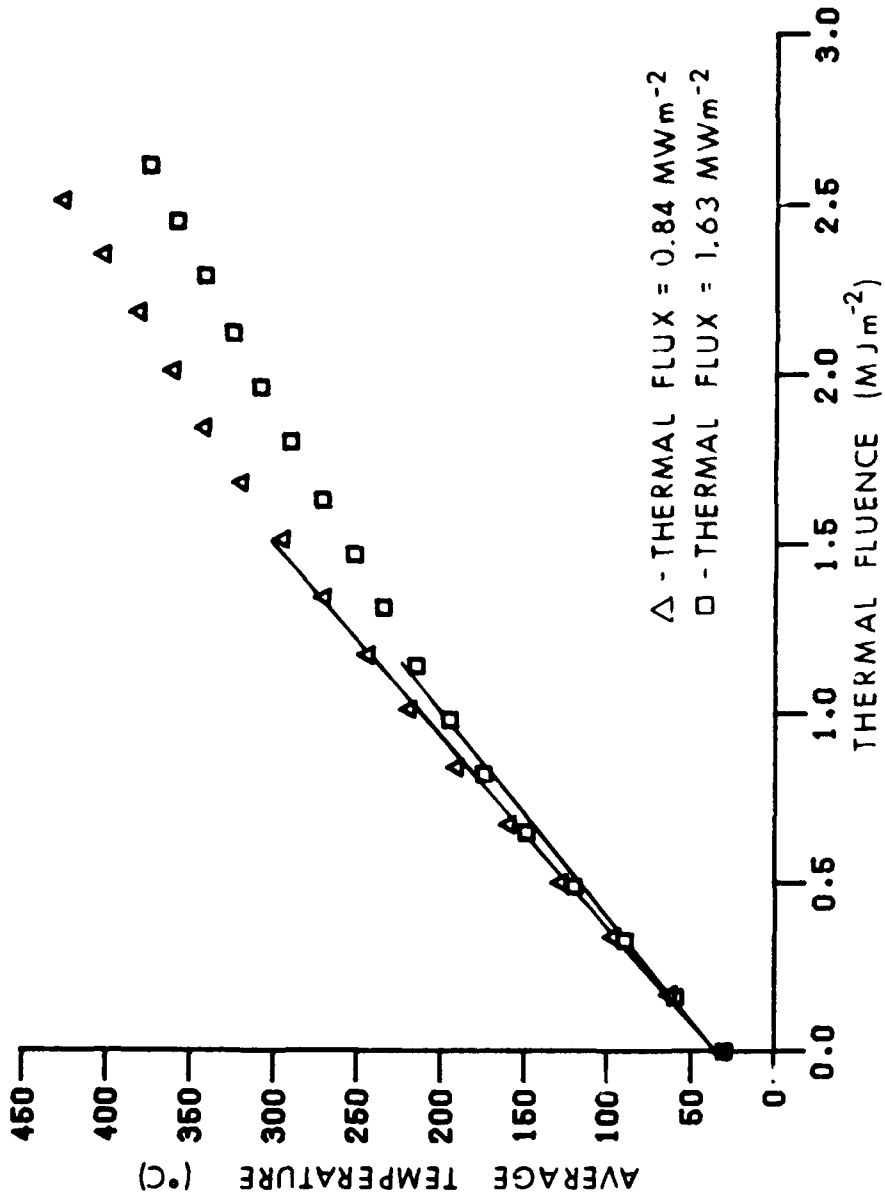


Figure 14. Sample D Average Temperature - Solar Furnace

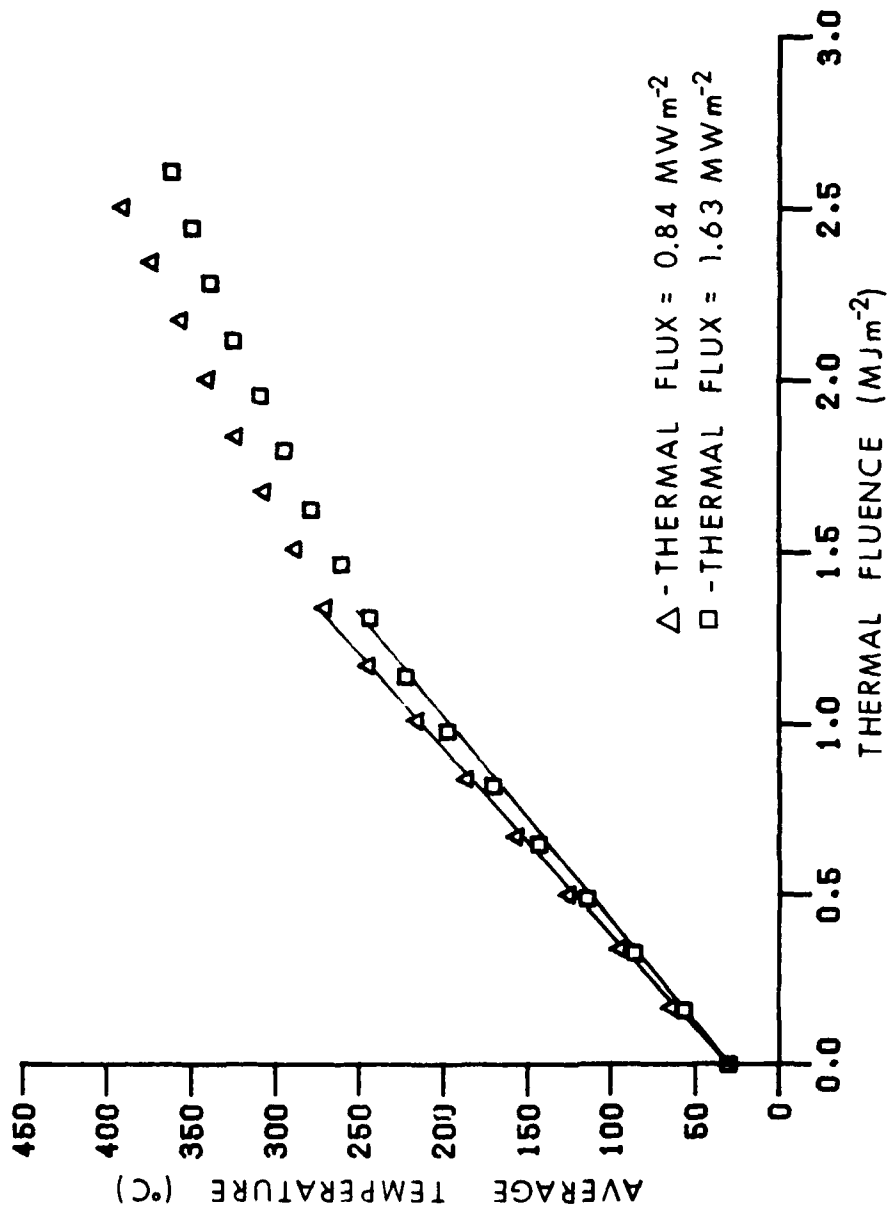


Figure 15. Sample E Average Temperature - Solar Furnace

It can be concluded from the test data that the effective absorptivities for all the Forest Green Camouflage paint-primer combinations have the same value, can be considered independent of temperature for temperatures less than 300°C, and may be independent of the thermal flux for the SF simulator.

Table 5 contains the flux values and effective absorptivity of all the samples for each simulator. The average effective absorptivity of all the samples for both flux values for each simulator is given by $\bar{\alpha}_e$

TABLE 5. Effective Absorptivity

Flux	Quartz Lamps	Solar Furnace
0.84 MW/m ²	0.47	0.66
1.59 MW/m ²	0.45	-
1.63 MW/m ²	-	0.62
$\bar{\alpha}_e$	0.46 ± 0.02	0.64 ± 0.02

The average effective absorptivity associated with the Solar Furnace simulator is 39% greater than the average effective absorptivity associated with the Quartz Lamps simulator.

IV. CONCLUSIONS

The amount of thermal energy absorbed by a system whose exposed surfaces are painted with a Forest Green Camouflage paint-primer combination is highly dependent on the thermal radiation spectrum and may be independent of the thermal radiation flux. Thirty-nine percent more energy was absorbed using the solar furnace than was absorbed using the quartz lamps. The implication of the dependence of the absorptivity on the thermal radiation spectrum is obvious. The survivability of a system to a simulated thermal or thermal-blast environment may be simulator dependent. Consequently, until it has been determined to what extent the nuclear thermal radiation environment must be simulated, system survivability results using thermal simulators are questionable.

APPENDIX A. Average Temperature Data

Table A1 gives the number of specimens of each paint-primer sample exposed at each simulator.

TABLE A1. Number of Paint-Primer Exposures

Sample	Quartz Lamps		Solar Furnace	
	0.84 MW/m^2	1.59 MW/m^2	0.84 MW/m^2	1.63 MW/m^2
A	5	5	3	5
B	5	5	4	5
C	5	5	3	5
D	5	5	3	4
E	5	5	4	4

Tables A2 through A5 list the thermal fluence, Q , and the average temperature, \bar{T}_i , with its standard deviation. The subscript of \bar{T} designates the sample and all temperatures and standard deviation were rounded off to the nearest degree.

TABLE A2. Average Temperatures for Quartz Lamps

Flux = 0.84 MW/m²

Q (MJ/m ²)	\bar{T}_A (°C)	\bar{T}_B (°C)	\bar{T}_C (°C)	\bar{T}_D (°C)	\bar{T}_E (°C)
0.00	30	30	30	30	30
0.17	53 ± 1	53 ± 1	52 ± 1	51 ± 1	52 ± 1
0.34	75 ± 1	76 ± 1	74 ± 1	72 ± 2	74 ± 2
0.50	98 ± 1	99 ± 1	96 ± 1	94 ± 1	95 ± 2
0.67	119 ± 2	122 ± 1	118 ± 1	116 ± 1	117 ± 1
0.84	144 ± 2	145 ± 2	139 ± 1	138 ± 1	139 ± 2
1.01	167 ± 1	168 ± 2	159 ± 2	159 ± 2	160 ± 2
1.17	189 ± 1	189 ± 1	182 ± 2	180 ± 1	182 ± 3
1.34	210 ± 2	212 ± 2	202 ± 1	203 ± 2	203 ± 2
1.51	235 ± 1	231 ± 2	220 ± 2	225 ± 2	221 ± 2
1.68	252 ± 2	254 ± 1	240 ± 2	246 ± 1	241 ± 2
1.84	271 ± 1	274 ± 2	259 ± 2	272 ± 1	261 ± 3
2.01	295 ± 2	294 ± 2	278 ± 2	297 ± 2	279 ± 3
2.18	315 ± 3	314 ± 2	298 ± 3	322 ± 3	297 ± 3
2.35	336 ± 3	334 ± 3	316 ± 3	349 ± 4	317 ± 4
2.51	347 ± 3	349 ± 4	*	*	*

* No data

TABLE A3. Average Temperatures for Quartz Lamps

Flux = 1.59 MW/m^2

$Q \text{ (MJ/m}^2\text{)}$	$\bar{T}_A \text{ (C)}$	$\bar{T}_B \text{ (C)}$	$\bar{T}_C \text{ (C)}$	$\bar{T}_D \text{ (C)}$	$\bar{T}_E \text{ (C)}$
0.00	30	30	30	30	30
0.16	49 \pm 2	52 \pm 1	48 \pm 2	49 \pm 1	48 \pm 1
0.32	68 \pm 3	71 \pm 1	68 \pm 2	68 \pm 2	68 \pm 1
0.48	88 \pm 4	92 \pm 2	87 \pm 1	87 \pm 2	88 \pm 1
0.64	108 \pm 4	113 \pm 2	106 \pm 1	107 \pm 1	107 \pm 2
0.80	127 \pm 4	131 \pm 1	127 \pm 2	128 \pm 2	128 \pm 2
0.96	148 \pm 6	153 \pm 2	145 \pm 1	148 \pm 3	148 \pm 2
1.11	168 \pm 6	174 \pm 2	164 \pm 2	168 \pm 3	165 \pm 3
1.27	185 \pm 7	193 \pm 1	183 \pm 2	188 \pm 3	185 \pm 2
1.43	206 \pm 7	214 \pm 1	201 \pm 2	209 \pm 3	205 \pm 2
1.59	222 \pm 8	232 \pm 2	219 \pm 1	232 \pm 5	225 \pm 2
1.75	238 \pm 9	252 \pm 2	237 \pm 2	254 \pm 4	242 \pm 2
1.91	264 \pm 10	273 \pm 3	256 \pm 3	276 \pm 5	258 \pm 3
2.07	276 \pm 12	289 \pm 2	273 \pm 3	299 \pm 6	278 \pm 3
2.23	290 \pm 12	308 \pm 3	291 \pm 3	321 \pm 7	296 \pm 3
2.39	299 \pm 12	325 \pm 4	309 \pm 4	343 \pm 8	314 \pm 4

TABLE A4. Average Temperatures for Solar Furnace

Flux = 0.84 MW/m^2

$Q \text{ (MJ/m}^2\text{)}$	$\bar{T}_A \text{ (C)}$	$\bar{T}_B \text{ (C)}$	$\bar{T}_C \text{ (C)}$	$\bar{T}_D \text{ (C)}$	$\bar{T}_E \text{ (C)}$
0.0	30	30	30	30	30
0.17	62 \pm 3	63 \pm 2	61 \pm 2	62 \pm 1	63 \pm 1
0.34	92 \pm 2	97 \pm 3	93 \pm 1	96 \pm 1	94 \pm 2
0.50	124 \pm 2	128 \pm 3	125 \pm 1	127 \pm 1	125 \pm 5
0.67	154 \pm 3	160 \pm 3	156 \pm 2	158 \pm 2	156 \pm 6
0.84	185 \pm 4	190 \pm 4	184 \pm 1	190 \pm 1	186 \pm 6
1.01	215 \pm 3	220 \pm 3	213 \pm 1	218 \pm 4	215 \pm 6
1.17	238 \pm 3	248 \pm 3	242 \pm 1	243 \pm 4	244 \pm 6
1.34	263 \pm 3	276 \pm 4	272 \pm 1	269 \pm 4	269 \pm 9
1.51	287 \pm 3	306 \pm 6	300 \pm 2	294 \pm 5	287 \pm 12
1.68	307 \pm 5	326 \pm 4	328 \pm 3	319 \pm 6	306 \pm 15
1.84	322 \pm 6	346 \pm 4	349 \pm 2	341 \pm 8	323 \pm 16
2.01	334 \pm 7	367 \pm 5	368 \pm 2	360 \pm 9	339 \pm 19
2.18	346 \pm 7	386 \pm 6	387 \pm 2	380 \pm 9	355 \pm 21
2.35	360 \pm 5	404 \pm 6	403 \pm 3	401 \pm 9	372 \pm 25
2.51	379 \pm 5	424 \pm 8	422 \pm 1	426 \pm 9	389 \pm 30

TABLE A5. Average Temperatures for Solar Furnace

Flux = 1.63 MW/m^2

$Q \text{ (MJ/m}^2\text{)}$	$\bar{T}_A \text{ (C)}$	$\bar{T}_B \text{ (C)}$	$\bar{T}_C \text{ (C)}$	$\bar{T}_D \text{ (C)}$	$\bar{T}_E \text{ (C)}$
0.00	30	30	30	30	30
0.16	60 \pm 4	59 \pm 3	58 \pm 1	59 \pm 1	56 \pm 3
0.33	91 \pm 4	92 \pm 3	87 \pm 2	89 \pm 2	86 \pm 6
0.49	120 \pm 5	121 \pm 4	117 \pm 3	120 \pm 3	114 \pm 8
0.65	150 \pm 6	150 \pm 5	145 \pm 2	148 \pm 2	143 \pm 9
0.82	180 \pm 7	180 \pm 5	176 \pm 4	174 \pm 3	170 \pm 11
0.98	205 \pm 6	210 \pm 1	205 \pm 3	195 \pm 3	197 \pm 14
1.14	226 \pm 7	235 \pm 5	231 \pm 3	215 \pm 3	222 \pm 15
1.31	247 \pm 8	261 \pm 7	259 \pm 3	234 \pm 4	243 \pm 13
1.47	268 \pm 8	283 \pm 9	285 \pm 2	252 \pm 4	260 \pm 13
1.63	287 \pm 8	304 \pm 9	307 \pm 3	271 \pm 2	278 \pm 15
1.80	304 \pm 8	328 \pm 9	327 \pm 3	290 \pm 3	294 \pm 16
1.96	316 \pm 8	339 \pm 10	345 \pm 5	308 \pm 3	309 \pm 16
2.12	327 \pm 8	354 \pm 13	362 \pm 6	325 \pm 4	324 \pm 18
2.29	343 \pm 10	363 \pm 14	378 \pm 7	341 \pm 3	338 \pm 19
2.45	357 \pm 12	387 \pm 12	393 \pm 10	358 \pm 3	349 \pm 21
2.61	372 \pm 14	402 \pm 11	412 \pm 10	375 \pm 3	361 \pm 21

DISTRIBUTION LIST

<u>No. of Copies</u>	<u>Organization</u>	<u>No. of Copies</u>	<u>Organization</u>
12	Commander Defense Technical Info Center ATTN: DDC-DDA Cameron Station Alexandria, VA 22314	1	Director US Army Air Mobility Research & Development Command Ames Research Center Moffett Field, CA 94035
1	Director Defense Nuclear Agency ATTN: STSS Washington, DC 20305	1	Commander US Army Communication Research & Development Command ATTN: DRDCO-PPA-SA Fort Monmouth, NJ 07703
1	Commander US Army Materiel Development & Readiness Command ATTN: DRCDMD-ST 5001 Eisenhower Avenue Alexandria, VA 22333	1	Commander US Army Electronics Research & Development Command Technical Support Activity ATTN: DELSD-L Fort Monmouth, NJ 07703
2	Commander US Army Armament Research & Development Command ATTN: DRDAR-TSS (2 cys) Dover, NJ 07801	1	Commander US Army Harry Diamond Lab ATTN: DELHD-NP 2800 Powder Mill Road Adelphi, MD 20783
1	Commander US Army Armament Material Readiness Command ATTN: DRSAR-LEP-L, Tech Lib Rock Island, IL 61299	1	Commander US Army Missile Command ATTN: DRSMI-R Redstone Arsenal, AL 35809
1	Director US Army ARRADCOM Benet Weapons Laboratory ATTN: DRDAR-LCB-TL Watervliet, NY 12189	1	Commander US Army Missile Command ATTN: DRSMI-YDL Redstone Arsenal, AL 35809
1	Commander US Army Aviation Research & Development Command ATTN: DRSAV-E P.O. Box 209 St. Louis, MO 61366	1	Commander US Army Mobility Equipment Research & Development Laboratory ATTN: DRDME-VD, J. Laffermen Fort Belvoir, VA 22060
		1	Commander US Army Tank Automotive Research & Development Command ATTN: DRDTA-UL Warren, MI 48090

DISTRIBUTION LIST

<u>No. of Copies</u>	<u>Organization</u>	<u>No. of Copies</u>	<u>Organization</u>
3	Commander White Sands Missile Range ATTN: STEWS-TE-AN, R. Hayes K. Cummings L. Flores White Sands Missile Range, NM 88002		<u>Aberdeen Proving Ground</u> Dir, USAMSAA ATTN: DRXSY-D DRXSY-MP, H. Cohen Cdr, USATECOM ATTN: DRSTE-TO-F
1	Commander US Army Nuclear Agency ATTN: MONA-WE, Dr.C. Davidson 7500 Backlick RD, Bldg 2073 Springfield, VA 22150		Dir, Wpns Sys Concepts Team Bldg E3516, EA ATTN: DRDAR-ACW Cdr, CSL Bldg E3330, EA ATTN: DRDAR-CLB-P B. Gerber J. Vervier A. Stuempfle DRDAR-CLB-CR J. Pistretto
1	Director US Army TRADOC Systems Analysis Activity ATTN: ATAA-SL, Tech Lib White Sands Missile Range NM 88002		
1	Commander Naval Surface Weapons Center ATTN: Code WR-42, N. Griff Silver Spring, MD 20910		
1	AFWL/SAT, A. Sharp Kirtland AFB, NM 87117		
1	Science Applications, Inc. ATTN: Dr.J. Cockayne 8400 Westpark Drive McLean, VA 22102		
1	University of Dayton Research Institute ATTN: Mr. N. Olsen Dayton, OH 45465		

USER EVALUATION OF REPORT

Please take a few minutes to answer the questions below; tear out this sheet and return it to Director, US Army Ballistic Research Laboratory, ARRADCOM, ATTN: DRDAR-TSB, Aberdeen Proving Ground, Maryland 21005. Your comments will provide us with information for improving future reports.

1. BRL Report Number _____

2. Does this report satisfy a need? (Comment on purpose, related project, or other area of interest for which report will be used.)

3. How, specifically, is the report being used? (Information source, design data or procedure, management procedure, source of ideas, etc.) _____

4. Has the information in this report led to any quantitative savings as far as man-hours/contract dollars saved, operating costs avoided, efficiencies achieved, etc.? If so, please elaborate.

5. General Comments (Indicate what you think should be changed to make this report and future reports of this type more responsive to your needs, more usable, improve readability, etc.) _____

6. If you would like to be contacted by the personnel who prepared this report to raise specific questions or discuss the topic, please fill in the following information.

Name: _____

Telephone Number: _____

Organization Address: _____

